

# Aperiodical oscillation of interlayer coupling in epitaxial Co/Ir(001) superlattices

H. Yanagihara\* and Eiji Kita

*Institute of Applied Physics and Center for Tsukuba Advanced Research Alliance (TARA), University of Tsukuba, Tsukuba, 305-8573 Japan*

M. B. Salamon

*Department of Physics, University of Illinois, Urbana, Illinois 61801*

(Received 12 May 1999)

High quality epitaxial cobalt-iridium superlattices were successfully grown on MgO(001) substrates via molecular-beam epitaxy and were found to exhibit anomalous oscillatory interlayer exchange coupling with a strong coupling constant. The aperiodical antiferromagnetic (AF) peaks appear at Ir layer thicknesses of 5 Å, 15 Å, and 33 Å. Maximum magnetoresistance (MR) ratios of  $\approx 1.1\%$  are obtained and are almost the same for the first and the second AF peaks. The interlayer coupling corresponding to the first AF peak is so strong that the magnetization did not saturate even in an applied field up to 90 kOe. The estimated value of the interlayer exchange constant by MR curves at room temperature is more than  $2.2 \text{ erg/cm}^2$  close to the first AF peak. A distinction of the in-plane magnetization process between [100] and [110] directions is observed and the easy axis of magnetization is found to be along the [110] axis in plane. The aperiodic oscillations are thought to indicate multiperiodicity of the interlayer exchange constants. [S0163-1829(99)01742-7]

## I. INTRODUCTION

Since the discovery<sup>1</sup> of interlayer coupling between adjacent ferromagnetic layers that oscillates with the thickness of nonmagnetic spacers, numerous experimental and theoretical studies of the effect have been reported. Many combinations of materials, in sandwiches and multilayers, have been examined in terms of their coupling and the oscillation periods.<sup>2</sup> In multilayers, the oscillation periods are between 8 Å and 12 Å for almost any metal spacer<sup>3</sup> and no multiperiodicity has been observed. From a theoretical perspective, the oscillation periods are found to be equal to  $2\pi/|\mathbf{q}_i|$ , where  $\mathbf{q}_i$  is one of the extremal spanning vectors that connects stable points of the Fermi surface of the spacer material along the growth direction.<sup>4-6</sup> Multiperiodicities that imply both short- (about 2 monolayers) and long-range (about 5–8 monolayers) periodicities of interlayer coupling have been reported in several well-controlled sandwich systems. In multilayer systems, however, short-range coupling oscillations have not been observed, despite theoretical predictions, presumably a consequence of interfacial roughness.<sup>4</sup> In general, in order to study interlayer coupling, most reports focused on noble metals or on  $3d$  transition metals, which show antiferromagnetism as spacer materials. Noble metals have rather simple Fermi surfaces where there are a few extremal spanning vectors, and less lattice misfit with a magnetic-layer element, so that one can easily compare theoretical predictions and experimental results; there are remarkable correspondences between theoretical and experimental oscillation periods.<sup>7</sup> Recently, Unguris *et al.*, using carefully grown Fe/Au/Fe trilayers, showed experimental results consistent in not only the periodicity, but also the magnitude of exchange coupling.<sup>8</sup> Unfortunately, there are fewer studies of superlattices consisting of  $4d$  or  $5d$  transition metals as a spacer, possibly because of the more complicated Fermi surface and prospective changes in electronic structure

caused by large lattice misfits between spacer metals and ferromagnetic metals. There are numerous spanning vectors on the Fermi surface of the transition metals, each of which may be associated with an oscillation period.<sup>6</sup> In the case of multilayers composed of transition metal spacers, we expect, therefore, to observe multiperiodicity consistent with two or more long-range periodicities.

Superlattices composed of a  $3d$  ferromagnetic metal (Co) and  $5d$  transition metal spacer (Ir) have been found to exhibit magnetic properties commonly observed in other ferromagnetic/transition or noble metal systems, i.e., perpendicular magnetic anisotropy,<sup>9</sup> and magnetic exchange coupling that depends on spacer layer thickness.<sup>3,10-12</sup> Although the interlayer coupling in Ir systems is much stronger than that in other  $3d$  or noble-metal systems [Co/Ir is reported to be the second strongest antiferromagnetic (AF) coupling system in Parkin's pioneering work<sup>3</sup>], there have been few reports of magnetic properties or superlattice structure. Recently, additional work on the Co/Ir multilayer systems has appeared, focusing on the interlayer coupling and magnetoresistance (MR).<sup>10,11</sup> However, the samples studied were made by sputtering method, so that the multilayers were composed of (111) preferred crystalline texture. In order to study interlayer coupling, it is much better to treat single crystal samples; that is, epitaxial superlattices. This poses an experimental challenge, as there is a large lattice misfit between fcc-Co and fcc-Ir, expected to be about 8%. In order to grow Co/Ir epitaxially, then, well-controlled and optimized growth conditions are necessary. In this paper, we report the growth of Co/Ir(001) superlattice structures prepared with molecular-beam epitaxy (MBE), and on the dependence of magnetic properties on Ir layer thickness.

## II. EXPERIMENT

All samples were grown at the University of Tsukuba using a conventional MBE system (SEO-5 made by Japan

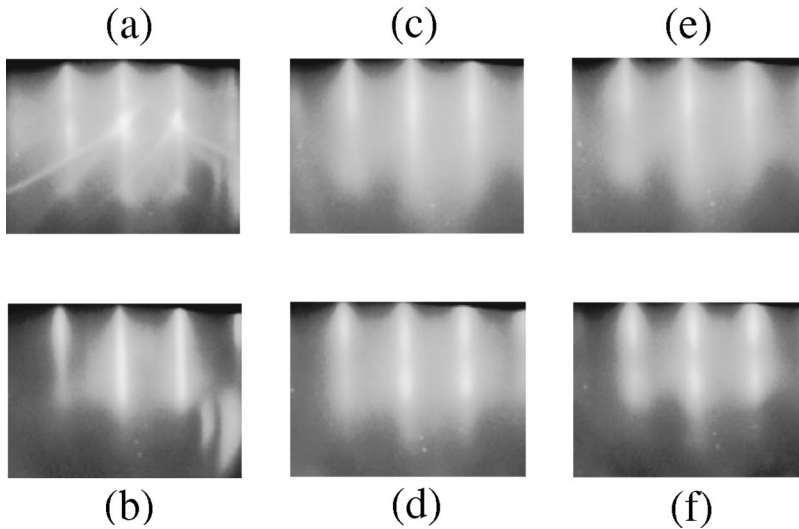


FIG. 1. RHEED patterns of a  $[\text{Co } 7 \text{ \AA}/\text{Ir } 11 \text{ \AA}](001)$  superlattice during the growth process. The incident electron beam is parallel to  $\text{MgO}[100]$  and accelerated to 15 kV. (a) After driving off the impurities by substrate heating. (b) Reflection pattern of Ir buffer layer. (c) The tenth Co layer. (d) The tenth Ir layer. (e) The fiftieth Co layer. (f) The fiftieth Ir layer. The final Ir layer thickness is 50  $\text{\AA}$  for prevention of oxidation.

SEED LAB. Ltd.), which includes reflected high-energy electron diffraction (RHEED) equipment. Single crystal  $\text{MgO}(001)$  substrates, polished for epitaxial growth, were used. Layer thickness and deposition rates for each source were monitored by crystal oscillator and controlled by a commercial deposition controller. Films for nominal thickness calibration were measured via multiple beam interferometry and contact step meter. The difference between both methods is negligible.

Prior to growth, the substrates were heated to  $600^\circ\text{C}$  for three hours or more in a growth chamber. Layers of 12  $\text{\AA}$  Fe and 50  $\text{\AA}$  Pt were subsequently grown on the  $\text{MgO}(001)$  substrate as seed layers at  $600^\circ\text{C}$  in order to relax the mismatch between  $\text{MgO}(001)$  substrates and  $\text{Ir}(001)$  buffer layers and to facilitate the growth of a flat surface.<sup>13</sup> After deposition of seed layers, an Ir layer of 500  $\text{\AA}$  was deposited at the same temperature. Growth rates were 0.1  $\text{\AA}/\text{sec}$ , 0.1  $\text{\AA}/\text{sec}$ , and 0.2  $\text{\AA}/\text{sec}$ , for Fe, Pt, and Ir, respectively. Co/Ir superlattices were grown at  $\approx 60^\circ\text{C}$  to suppress alloying and interdiffusion. The deposition rate was controlled to be  $0.15 \pm 0.02 \text{ \AA}/\text{sec}$ . A series of superlattices were designed with fixed Co layer thickness of 7  $\text{\AA}$ , while Ir layer thicknesses were varied nominally from 5  $\text{\AA}$  to 40  $\text{\AA}$ . The repetition number of bilayers for each sample was 50 and a final 50- $\text{\AA}$ -thick Ir layer was deposited in order to prevent oxidation. The base pressure of the deposition chamber was approximately  $1 \times 10^{-9}$  torr and the typical deposition pressure was better than  $4 \times 10^{-8}$  torr during superlattice growth. We determined each layer thickness using intervals of superlattice peaks obtained by x-ray diffraction patterns by fitting the slope and intercept of the superlattice intervals versus nominal Ir layer thickness. The intercept and the slope correspond respectively to the Co layer thickness and the Ir layer correction factor between nominal and actual thickness. The obtained intercept (Co layer thickness) is around 6.7  $\text{\AA}$  and the slope is 0.9. While the difference of Co layer thickness between nominal and that estimated by the intervals is less than 5%, we denote the Co thickness as 7  $\text{\AA}$ . On the other hand, the difference for the Ir layers is not negligible, and we express the rounded off thickness after correction by the factor 0.9 in the following.

The structure of superlattices was examined *in situ* with RHEED and *ex situ* with x-ray diffractometry by  $\text{Cu-K}\alpha$  radiation. The RHEED patterns were recorded on photo-

graphic films. In order to measure MR, samples were cleaved along  $\text{MgO}\langle 100 \rangle$  and  $\langle 010 \rangle$  directions, and were shaped in a rectangle  $\sim 2 \times 8 \text{ mm}^2$  in size. MR measurements were carried out at room temperature and magnetic fields were applied in plane up to 15 kOe in usual cases; some samples, which show high saturation fields, were measured up to 90 kOe. Both the measurement current of 0.1 mA and typical applied magnetic fields were parallel to the in-plane  $\text{MgO}[100]$ . Magnetization measurements were performed at room temperature with a commercial superconducting quantum interference device magnetometer with magnetic fields up to 50 kOe applied mainly along the in-plane  $\text{MgO}[100]$ .

### III. RESULTS AND DISCUSSIONS

Figure 1 shows RHEED patterns of each step during the growth of  $[\text{Co } 7 \text{ \AA}/\text{Ir } 11 \text{ \AA}]_{50}(001)$ . The RHEED pattern shown in Fig. 1(a) is the  $\text{MgO}(001)$  substrate after heating for 3 h. At first, the pattern of seed layer Fe growth appears as smeary spots. After deposition of 50  $\text{\AA}$  Pt, the patterns become broad streaks, meaning that a flat film surface has developed. Figure 1(b) shows the pattern of the 500  $\text{\AA}$  Ir buffer layer. The sharp streak pattern of Ir buffer layers grown over 300  $\text{\AA}$  indicates a sufficiently flat surface. We could not observe a  $5 \times 1$  surface reconstruction of Ir (001) from the pattern of 500- $\text{\AA}$ -thick Ir layer. The crystal relationship  $\text{MgO}[100](001) \parallel \text{Ir}[100](001)$  is deduced from these RHEED patterns.

The RHEED patterns from the tenth Co layer, the tenth Ir layer, the final (50th) Co layer, and Ir capping layer are shown in Figs. 1(c), 1(d), 1(e), 1(f), respectively. No remarkable change of RHEED pattern, except the brightness, was observed in the whole process of the superlattice growth, that is, from the first Co layer deposition to the final Ir layer deposition. The streak patterns indicate that the growth mode of superlattices is layer-by-layer-like growth. During Co layer growth, the streak patterns blur a little and their brightness dims. On the other hand, during Ir layer growth, the streak patterns tend to brighten and slightly shorten. This tendency was observed in all samples.

X-ray diffraction patterns of some samples comprised of different Ir layer thicknesses are shown in Fig. 2. A strong,

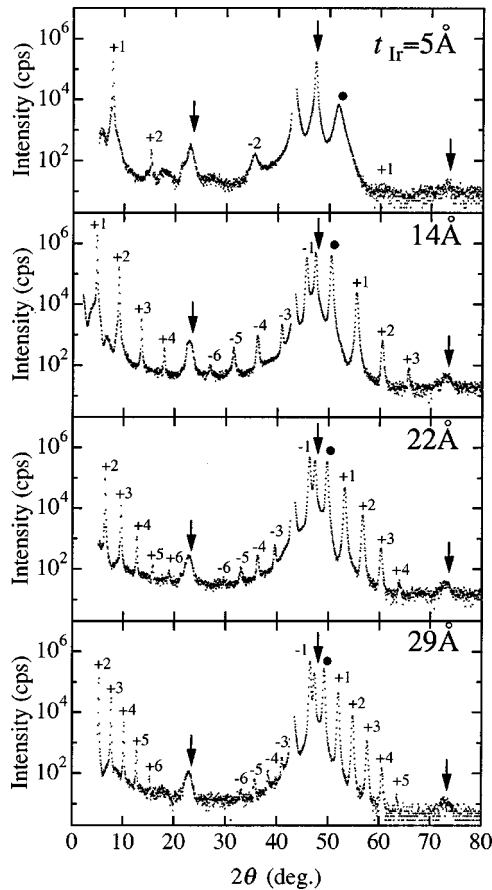


FIG. 2. X-ray diffraction patterns of Co 7 Å/Ir ( $t_{\text{Ir}}$ ) Å(001) superlattice. The  $t_{\text{Ir}}$ 's value is denoted in each figure.

sharp peak placed at  $2\theta \approx 47.4^\circ$  originates from the buffer Ir layer. Weak, broad peaks around  $2\theta \approx 20^\circ$  and  $2\theta \approx 74^\circ$  are contributions from the seed layers considered as FePt ordered alloy. Superlattice peaks are observed in the whole region from small to high angle; however, there is no evidence of (011) or (111) stacking in any samples. In the case of [Co 7 Å/Ir 14 Å]<sub>50</sub>(001), the full width at half maximum of a Co/Ir(002) peak is less than  $0.35^\circ$ , which yields a crystal coherence length larger than 250 Å. The existence of sharp and higher-order satellite peaks indicates that the superlattices have clear and sharp interfaces with little interface mixing and high superlattice periodicity.

Co thin films have the possibility of two different metastable crystalline structures at room temperature, i.e., fcc phase and bcc phase. It is believed that film growth conditions and growth orientation decide the Co structure. If a Co layer has bcc structure, the lattice misfit between fcc-Ir and bcc-Co is expected to be  $\approx +4\%$ ,<sup>14</sup> while in the case of fcc-Co, the misfit is  $\approx -8\%$ . In the step model of x-ray diffraction (XRD) pattern analysis of superlattices,<sup>15</sup> the intensity of superlattice peaks is mainly determined by the form-factor envelopes of the layers that comprise each bilayer. Although the superlattice peaks around Ir(002) appear to be composed of only one envelope (because the two envelopes for Co and Ir layers are close to each other), the peaks around (004) are composed of two distinguishable envelopes. The center of one envelope coincides with the peak of buffer Ir(004) and the other one is close to fcc-Co(004) but at an obviously larger angle position. If we suppose that

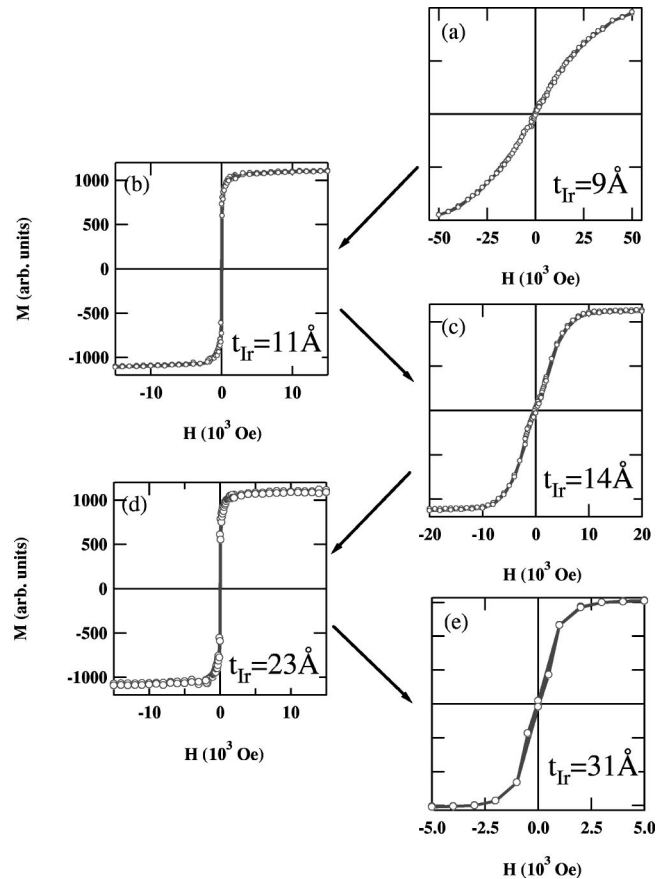


FIG. 3. Typical  $MH$  curves of Co 7 Å/Ir ( $t_{\text{Ir}}$ ) Å(001) superlattices at room temperature. The  $t_{\text{Ir}}$  are given in the figure. In samples designed with thin Ir thickness, the magnetization does not saturate even at 90 kOe.

the Co layer has bcc structure, the envelope center could not be observed in this region. The XRD profiles around the (004) reflection support the picture of fcc-Co diminished along the growth direction. Our preliminary results of off-axis x-ray diffraction measurements using a four circle diffractometer also support fcc structure of Co layers.

Figure 3 shows some typical  $MH$  curves of [Co 7 Å/Ir( $t_{\text{Ir}}$ )]<sub>50</sub>(001) measured at room temperature. From the results of in-plane and perpendicular magnetization processes, it is found that the easy axis of magnetization lies in the film plane irrespective of the Ir layer thickness. All samples designed with  $t_{\text{Ir}} < 9$  Å show little remanence, and have such remarkably high saturation fields ( $H_s$ ) that we could not saturate their magnetization even in  $H = 50$  kOe. This behavior means that the adjacent Co layers couple strongly antiferromagnetically and the layer structures of the superlattices must be sufficiently perfect that direct coupling between adjacent Co layers is negligible even for Ir layer thickness of only 2–5 monolayers. The shape of the  $MH$  curves is strongly dependent on Ir layer thickness. The squareness [a ratio of the remanence ( $M_R$ ) to the saturation magnetization ( $M_S$ )] and the saturation field ( $H_S$ ) are strongly related to each other. The samples around  $t_{\text{Ir}} = 15$  Å, corresponding to the second AF peak, show typical, ideal antiferromagnetically coupled  $MH$  curves, with little remanence, high saturation field, and constant susceptibility. On the other hand,  $MH$  curves of the samples around  $t_{\text{Ir}} = 11$  Å

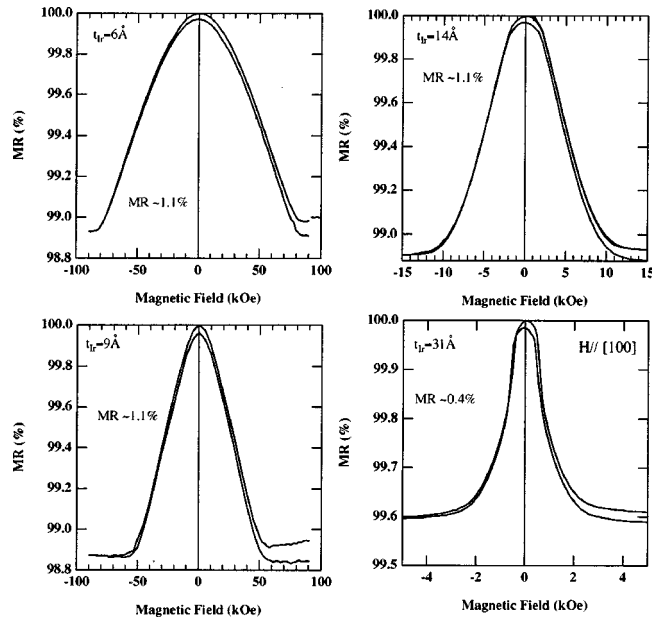


FIG. 4. MR curves of Co/Ir(001) superlattices with high saturation field and little remanence.

or  $t_{\text{Ir}} = 23 \text{ \AA}$  show large remanence and low saturation field. They are typical of ferromagnetically coupled or noncoupled hysteresis curves.

The MR curves for antiferromagnetically coupled superlattices are shown in Fig. 4, measured at room temperature with the applied field and current parallel to the [100] direction. Samples designed with Ir layer thickness thinner than  $9 \text{ \AA}$  were measured up to 90 kOe and the others were measured up to 15 kOe. All samples were saturated at fields lower than 90 kOe except those films with the thinnest Ir layer thickness; i.e.,  $t_{\text{Ir}} = 5 \text{ \AA}$ . Rounded shapes at low field and little hysteresis in the MR curves indicate ideal antiparallel alignment of the magnetic moments of adjacent Co layers at low field. The MR ratios at the first and the second AF peaks are about 1.1%. On the other hand, MR ratios of ferromagnetically coupled samples are very small, for instance, typically less than 0.1%. This MR value is larger than previous reports<sup>10-12</sup> on Co/Ir multilayers prepared by sputtering on thinner buffer layers. The saturation field  $H_S$  estimated from MR curves agrees well with that estimated from  $MH$  curves at the second and the third AF peaks, so it is reasonable to believe that we determined  $H_S$  from the MR curve of the thinner Ir samples with high  $H_S$ .

The magnetization process is dependent on the direction of the applied field, the magnetocrystalline anisotropy, and coupling strength, including its sign, between adjacent ferromagnetic layers. In the cubic case, samples have fourfold symmetry in the film plane. The easy axis is expected to be parallel to either [100] or [110] directions. The magnetization process along different directions for superlattices at the third AF peak is shown in Fig. 5. The measurements were carried out at room temperature and MR and  $MH$  curves of  $t_{\text{Ir}} = 31 \text{ \AA}$  sample were obtained along [110] and [100] directions. In both MR and  $MH$  curves, a clear difference is found. Slopes of the magnetization curve for  $H \parallel [110]$  and  $H \parallel [100]$  look similar at low field. They jump at almost the

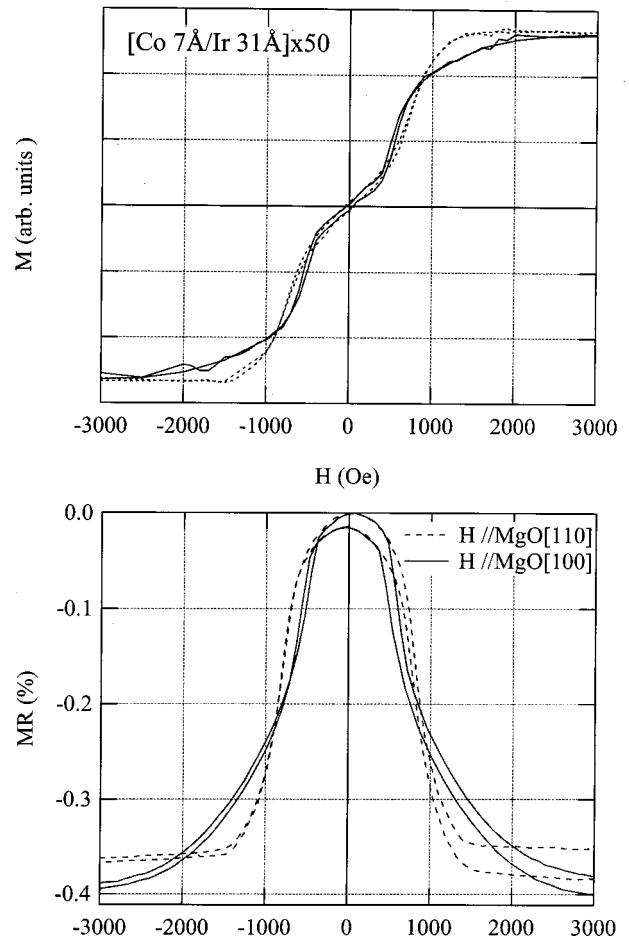


FIG. 5.  $MH$  and MR curves measured along [100] and [110] in plane for  $[\text{Co } 7 \text{ \AA} / \text{Ir } 31 \text{ \AA}]_{50}(001)$  superlattices. The upper figure shows  $MH$  curves obtained with applied field parallel to [100] (solid line) and [110] (broken line). The bottom figure shows MR curves measured with applied field parallel to [100] (solid line) and [110] (broken line).

same field of  $H \sim 500 \text{ Oe}$ . The magnetization curve for  $H \parallel [110]$  saturates at around 1400 Oe, while the magnetization for  $H \parallel [100]$  does not saturate and saturate below 3 kOe. The difference in  $MH$  curves of  $t_{\text{Ir}} = 31 \text{ \AA}$  along [100] and [110] directions implies that this superlattice shows an ideal magnetization process with competition between cubic anisotropy and antiferromagnetic coupling.<sup>16</sup> The inflection points at  $H \sim 500 \text{ Oe}$  indicate that two different magnetization jumps occur for the two  $MH$  loops, respectively; that is, a spin-flop type jump occurs in the [110]  $MH$  loop and a nonsymmetric-type jump occurs in the [100]  $MH$  loop. The easy axis in fcc-Co is known to be parallel to the [111] direction and the [110] axis is harder than the [111], but easier than [100].<sup>17</sup> Taking demagnetization fields into account, it is reasonable that the easy axis is parallel to the [110] in plane.

Other antiferromagnetically coupled samples, designed with thinner Ir layer thickness than above, around  $t_{\text{Ir}} = 5 \text{ \AA}$  or  $t_{\text{Ir}} = 15 \text{ \AA}$ , displayed inflection points in the  $MH$  curves reminiscent of spin-flop type or nonsymmetric-type magnetization jump, but we could not observe a clear distinction between the two directions in the film plane. If a large

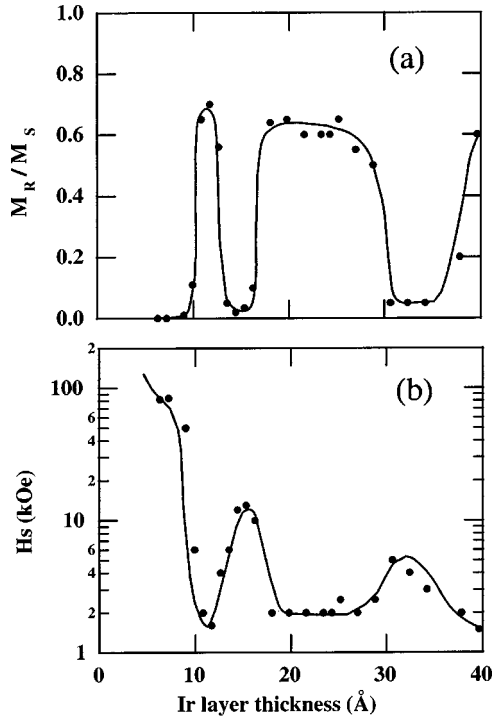


FIG. 6. The Ir layer thickness dependence of the AF coupling oscillation. (a) The  $t_{\text{Ir}}$  dependence on squareness of Co/Ir(001) superlattices. (b) The  $t_{\text{Ir}}$  dependence on saturation field of Co/Ir(001) superlattices.

difference exists between the AF coupling and the magnetocrystalline anisotropy energies, the  $MH$  curves are dominated by the stronger term. Evidently the magnetocrystalline anisotropy is so much smaller than the strong interlayer coupling that no clear difference is observed between the magnetization processes for different directions.

Figure 6 shows the Ir thickness dependence of the saturation field and normalized remanence at room temperature of Co/Ir (001) superlattices. The saturation fields were determined by the  $MH$  and MR measurements along the hard axis,  $H \parallel [100]$ . As mentioned above, in the thinner Ir samples the saturation fields obtained along  $[100]$  and  $[110]$  look very similar to each other because the saturation field is almost completely dominated by strong AF coupling. An unusual striking inharmoniously is found in both normalized remanence (squareness) plot and saturation field ( $H_s$ ) plot. The intervals between AF peaks in the Ir thickness dependence of  $H_s$  or between valleys in the squareness plot of the Ir thickness dependence reveal an irregular period of antiferromagnetic coupling oscillations. The samples with Ir layer thicknesses near 5 Å–7 Å possess a very strong antiferromagnetic coupling constant  $J \approx 2 \text{ erg/cm}^2$  at  $t_{\text{Ir}} = 6 \text{ Å}$ , while the system must become ferromagnetic in the limit  $t_{\text{Ir}} \rightarrow 0$ . Here, we suppose that the coupling constant can be expressed as  $J = H_s M_{\text{Co}} t_{\text{Co}} / 4$  and that the anisotropy energy is negligible. The sample with thinnest Ir layer thickness ( $t_{\text{Ir}} = 5 \text{ Å}$ ) possesses a saturation field in excess of 90 kOe, corresponding to  $J \geq 2.2 \text{ erg/cm}^2$ . This estimated coupling strength is exceeded only by the Co/Ru system.<sup>18</sup>

In many magnetic multilayer and sandwich systems that show interlayer exchange coupling, the coupling oscillation results in periodic AF peaks or MR maxima, and its oscilla-

tion periods are generally 10–20 Å for long periods and around 4 Å for short periods. From theoretical considerations, the dependence of the coupling energy on spacer thickness can be expressed in the following general form:

$$J_n = \frac{1}{n^2} \sum_m A_m \sin(2\pi n/\lambda_m + \phi_m),$$

where  $n$  is the spacer thickness in monoatomic layer units and  $m$  denotes spanning vectors that contribute to interlayer coupling. The wavelength  $\lambda_m$  corresponds to one of the oscillation periods and  $\phi_m$  is a characteristic phase of each oscillation period. As we mentioned in Sec. I, multiperiodicity has previously been found only in sandwich systems with noble metal spacers. Short period oscillations have not usually been found in multilayer systems because of the imperfections of layer structure, e.g., accumulative interface roughness and/or discrete thickness fluctuations.<sup>4</sup> We have observed three AF coupling peaks at around  $t_{\text{Ir}} = 5, 15,$  and  $33 \text{ Å}$  in 5–40 Å region. Compared with previous reported multilayer systems, present Co/Ir(001) system behaves peculiarly in terms of its oscillation periods; i.e., the AF peaks do not appear periodically. According to the calculation by Stiles,<sup>6</sup> the longest period is about 10 monolayer ( $\sim 19 \text{ Å}$ ). Although this value corresponds well to the spacing between the second and the third AF peaks found in our result, it is hard to elucidate the origin of the first AF peaks without considering multiperiodicity because no AF peak, associated with the first AF peak, occurs around 20–28 Å. Superposition of several periodicities with periods close to each other could also explain this peculiarity. In any case, it is necessary to explain this aperiodic oscillation by introducing multiperiodicity to multilayer system. The band structure of Ir, which belongs to the  $5d$  transition metal group is not so simple, even in the bulk state, so that many spanning vectors could exist along the  $[001]$  direction.<sup>6,19</sup> Although this aperiodic coupling oscillation is likely to be associated with multiperiodicity originating in the complicated Ir band structure, we cannot consider its band structure to be that of the bulk because of the large misfit. We believe these peculiarities are not features of only this system but would be found in other high-quality superlattices with  $4d$  or/and  $5d$  transition metal spacers. We would like to encourage theoretical investigation.

#### IV. CONCLUSION

We succeeded in the growth of high-quality Co/Ir(001) epitaxial superlattices via MBE. Co and Ir layers both possess fcc structure. The magnetic easy axis lies in plane for all samples and the easy axis is parallel to the  $[110]$  direction. MR ratios are small, even for AF coupled samples, while the coupling constants were particularly strong compared with other typical systems. The most interesting result is the aperiodic coupling oscillation, which may be due to a superposition of several periods corresponding to spanning vectors of the complicated Ir Fermi surface. In order to make clear these peculiarities, i.e., strong AF coupling and aperiodic coupling oscillation, further studies on sandwich samples with thicker Ir layers are in progress.

## ACKNOWLEDGMENTS

We would like to thank Dr. T. Taniyama and Dr. I. Nakatani at NRIM for MR measurement by PPMS and to K. Ono at University of Tsukuba for sample growth. One of the authors (H.Y.) would like to acknowledge Dr. T. Katayana, Dr. Y. Suzuki, and Dr. S. Yuasa at ETL for helpful discus-

sions. This study was partially supported by Grant-in-Aid for Scientific Research on Priority Areas (No. 10130204), and by a Distinguished Visiting Professorship (M.S.), from the Japan Ministry of Education, Science, Sports, and Culture. Partial support was received from the U.S. Department of Energy under Grant No. DEFG02-91ER45439.

\*Present address: Dept. of Physics, University of Illinois at Urbana-Champaign, Urbana, IL 61801.

<sup>1</sup>J. Kwo, E. M. Gyorgy, D. B. McWhan, M. Hong, F. J. DiSalvo, C. Vettier, and J. E. Bower, *Phys. Rev. Lett.* **55**, 1402 (1985); C. F. Majkrzak, J. W. Cable, J. Kwo, M. Hong, D. B. McWhan, Y. Yafet, J. V. Waszczak, and C. Vettier, *ibid.* **56**, 2700 (1986); P. Grünberg, R. Schreiber, Y. Pang, M. B. Brodsky, and H. Sowers, *ibid.* **57**, 2442 (1986).

<sup>2</sup>For a review, see in *Ultrathin Magnetic Structures II*, edited by J. A. C. Bland and B. Heinrich (Springer, Berlin, 1994).

<sup>3</sup>S. S. P. Parkin, *Phys. Rev. Lett.* **67**, 3598 (1991).

<sup>4</sup>P. Bruno and C. Chappert, *Phys. Rev. Lett.* **67**, 1602 (1991); **67**, 2592(E) (1991).

<sup>5</sup>P. Bruno, *Phys. Rev. B* **52**, 411 (1995).

<sup>6</sup>M. D. Stiles, *Phys. Rev. B* **48**, 7238 (1993).

<sup>7</sup>A. Fert and P. Bruno, in *Ultrathin Magnetic Structures II* (Ref. 2), Sec. 2, p. 82.

<sup>8</sup>J. Unguris, R. J. Celotta, and D. T. Pierce, *Phys. Rev. Lett.* **79**, 2734 (1997).

<sup>9</sup>F. J. A. den Broeder, W. Hoving, and P. J. H. Bloemen, *J. Magn. Mater.* **93**, 562 (1991).

<sup>10</sup>Y. Luo, M. Moske, and K. Samwer, *Europhys. Lett.* **42**, 565 (1998).

<sup>11</sup>A. Dinia, M. Stoeffel, K. Rahmouni, D. Stoeffler, and H. A. M. van den Berg, *Europhys. Lett.* **42**, 331 (1998).

<sup>12</sup>H. Yanagihara, K. Pettit, M. B. Salamon, Eiji Kita, and S. S. P. Parkin, *J. Appl. Phys.* **81**, 5197 (1997).

<sup>13</sup>R. F. C. Farrow, G. R. Harp, R. F. Marks, T. A. Rabedeau, M. F. Toney, D. Weller, and S. S. P. Parkin, *J. Cryst. Growth* **133**, 47 (1993).

<sup>14</sup>G. A. Prinz, *Phys. Rev. Lett.* **54**, 1051 (1985).

<sup>15</sup>Y. Fujii, in *Metallic Superlattices, Artificially Structured Materials*, edited by T. Shinjo and T. Takada (Elsevier, New York, 1987), p. 33ff.

<sup>16</sup>B. Dieny, J. P. Gavigan, and J. P. Rebouillat, *J. Phys.: Condens. Matter* **2**, 159 (1990).

<sup>17</sup>T. Suzuki, D. Weller, C.-A. Chang, R. Savoy, T. Huang, B. A. Gurney, and V. Speriosu, *Appl. Phys. Lett.* **64**, 2736 (1994).

<sup>18</sup>S. S. P. Parkin, N. More, and K. P. Roche, *Phys. Rev. Lett.* **64**, 2304 (1990).

<sup>19</sup>O. Krogh Anderson, *Phys. Rev. B* **2**, 883 (1970).